Applied Surface Science 364 (2016) 604–612

Contents lists available at ScienceDirect

Applied Surface Science

journal homepage: www.elsevier.com/locate/apsusc

Fabrication of novel magnetically separable $BiOBr/CoFe_2O_4$ microspheres and its application in the efficient removal of dye from aqueous phase by an environment-friendly and economical approach

R. Jiang[a,b,c], H.-Y. Zhu[a,b,c,*], J.-B. Li[b], F.-Q. Fu[a], J. Yao[a,c], S.-T. Jiang[c], G.-M. Zeng[d,**]

[a] Zhejiang Provincial Key Laboratory of Plant Evolutionary Ecology and Conservation, Taizhou University, Taizhou, Zhejiang 318000, PR China
[b] Environmental Engineering Program, University of Northern British Columbia, Prince George, British Columbia, Canada V2N 4Z9
[c] Department of Environmental Engineering, Taizhou University, Taizhou, Zhejiang 318000, PR China
[d] Key Laboratory of Environmental Biology and Pollution Control (Hunan University), Ministry of Education, Changsha 410082, PR China

ARTICLE INFO

Article history:
Received 19 September 2015
Received in revised form
23 December 2015
Accepted 26 December 2015
Available online 29 December 2015

Keywords:
Bismuth oxybromide
Cobalt ferrite
Photocatalysis
Decolorization
Congo red
Magnetic separation

ABSTRACT

Novel magnetically separable $BiOBr/CoFe_2O_4$ microspheres assembled from nanoparticles were successfully fabricated by a facile solvothermal method at 160 °C for 12 h. Then, $BiOBr/CoFe_2O_4$ microspheres were characterized via XRD, TEM, SEM, EDS and VSM. Congo red (CR) was selected as a pollutant model to evaluate the photocatalytic activities of $BiOBr/CoFe_2O_4$ microspheres. The value of coercivity (232 Oe) and the saturation magnetization (33.79 emu g^{-1}) were obtained, which indicated that $BiOBr/CoFe_2O_4$ microspheres can be separated and recovered easily from the treated solution. What is more, by calculation, the initial rate constants of $BiOBr/CoFe_2O_4$ microspheres is about 1.45 times higher than that of the

attracted great attention due to its obvious advantages of large saturation magnetization, good chemical stability, low cost, and

netization of novel materials based on $CoFe_2O_4$ nanoparticles allows fast and effective separation of those materials from aqueous solution by a magnet [30,39,40]. In addition, enhanced visible-light-driven photoactivity has been observed over some composite semiconductors which combine $CoFe_2O_4$ with secondary material, such as TiO_2 [33], Ag/AgCl [26] and Pd (0) [41]. Furthermore, conventional porous structure of $CoFe_2O_4$ nanoparticles provides effective sites for removal of pollutants in aqueous solution [30,39,42,43]. Therefore, considering the advantages of both excellent photocatalytic performance

for

solution

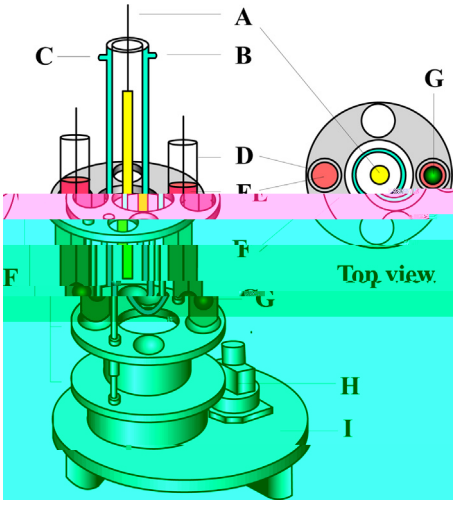

Fig. 1. Reactor used in the photocatalytic experiments. A. xenon lamp; B. cooling water inlet; C. cooling water outlet; D. quartz reactor; E. dye solution; F. rotating disks; G. aeration head; H. electric machinery; and I. pedestal.

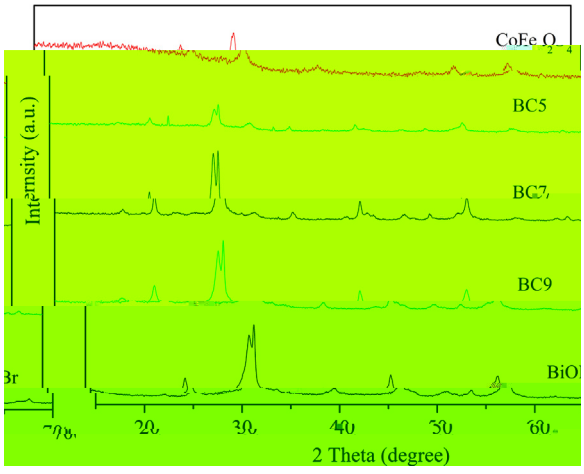

Fig. 2. XRD patterns of BiOBr, $CoFe_2O_4$ and BiOBr/$CoFe_2O_4$ microspheres.

Decolorization efficiency (η) of CR solution by BiOBr/$CoFe_2O_4$ microspheres at time t was calculated by Eq. (1).

$$\eta(\%) = \frac{(C_0 - C_t)}{C_0} \times 100 \quad (1)$$

where C_0 and C_t (mg L^{-1}) are the initial CR concentration and the CR concentrations at any time t (min), respectively.

3. Results and discussion

3.1. Characterization of as-synthesized samples

3.1.1. XRD

The phase structure of the as-prepared BiOBr, $CoFe_2O_4$ and BiOBr/$CoFe_2O_4$ microspheres were investigated by XRD analysis (Fig. 2). It can be easily found that the diffraction peaks on $CoFe_2O_4$ at $2\theta = 30.03°$, 35.48°, 43.03°, 56.94° and 62.49° were completely matched the reflections of (2 2 0), (3 1 1), (4 0 0), (5 1 1) and (4 4 0), respectively, indexed to the cubic spinel structure of $CoFe_2O_4$ (JCPDS 22-1086) [29,40,44]. The mean size of the $CoFe_2O_4$ crystallites calculated from the diffraction patterns was about 21 nm. The pure BiOBr sample showed a tetragonal crystal phase with the detected reflections at 22.13° (0 0 2), 25.21° (1 0 1), 31.69° (1 0 2), 32.27° (1 1 0), 39.35° (1 1 2), 46.29° (2 0 0), 50.7° (1 0 4) and 57.25°

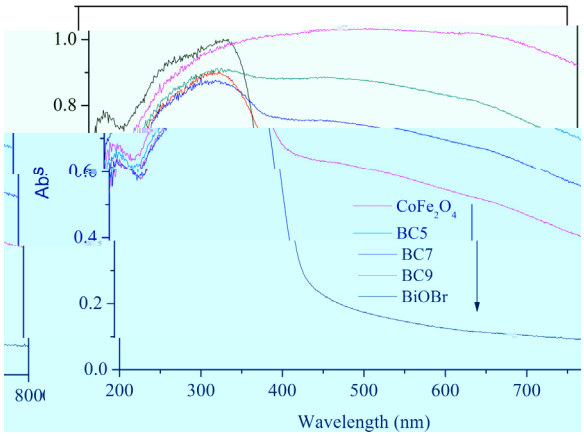

Fig. 3. UV–vis DRS of BiOBr, $CoFe_2O_4$ and BiOBr/$CoFe_2O_4$ microspheres.

(2 1 2) (JCPDS 78-0348) [16,19,44,45]. No crystalline $CoFe_2O_4$ can be detected from the BC9 with low $CoFe_2O_4$ concentrations, whereas two main peaks of $CoFe_2O_4$ at $2\theta = 35.28°$ (3 1 1) and 62.49° (4 4 0) were found from XRD patterns of BC7 and BC5, indicating the coexistence of $CoFe_2O_4$ and BiOBr in BC7 and BC5. In addition, the peak of BiOBr decreased gradually in intensity with the increase of $CoFe_2O_4$ content. The XRD diffraction of BC5 shows small impurities at $2\theta = 27.27°$, indicating that there is a small amount of impurity coexisting with diffraction of $CoFe_2O_4$ and BiOBr.

3.1.2. UV–Vis DRS

It is well known that the photoinduced charge-transfer property and enhanced light photocatalytic activity of semiconductors in the photocatalytic reaction are closely related to their optical properties [46]. Thus, the optical absorbance of as-prepared photocatalyst was measured by UV–visible diffuse reflectance spectra (DRS). The corresponding results are shown in Fig. 3. Obviously, pure BiOBr only has weak absorption in visible light region with an absorption edge around 442 nm and has a band gap of 2.81 eV, which is slightly larger than the values reported in previous literatures [11,13]. However, the absorption intensity of $CoFe_2O_4$ is very strong in both visible light and UV region from 200 nm to 800 nm, which results from the black appearance of pure $CoFe_2O_4$ material [26]. With the increase of $CoFe_2O_4$ content, the absorption in visible light region increased obviously and strengthened gradually due to the strong visible light response of $CoFe_2O_4$. The result is in agreement with the color change of the samples from yellow to black. In previous study, an obvious red-shift was also observed when BiOBr microsphere formed a heterojunction with other black materials [24]. The excel photocatalytic activity

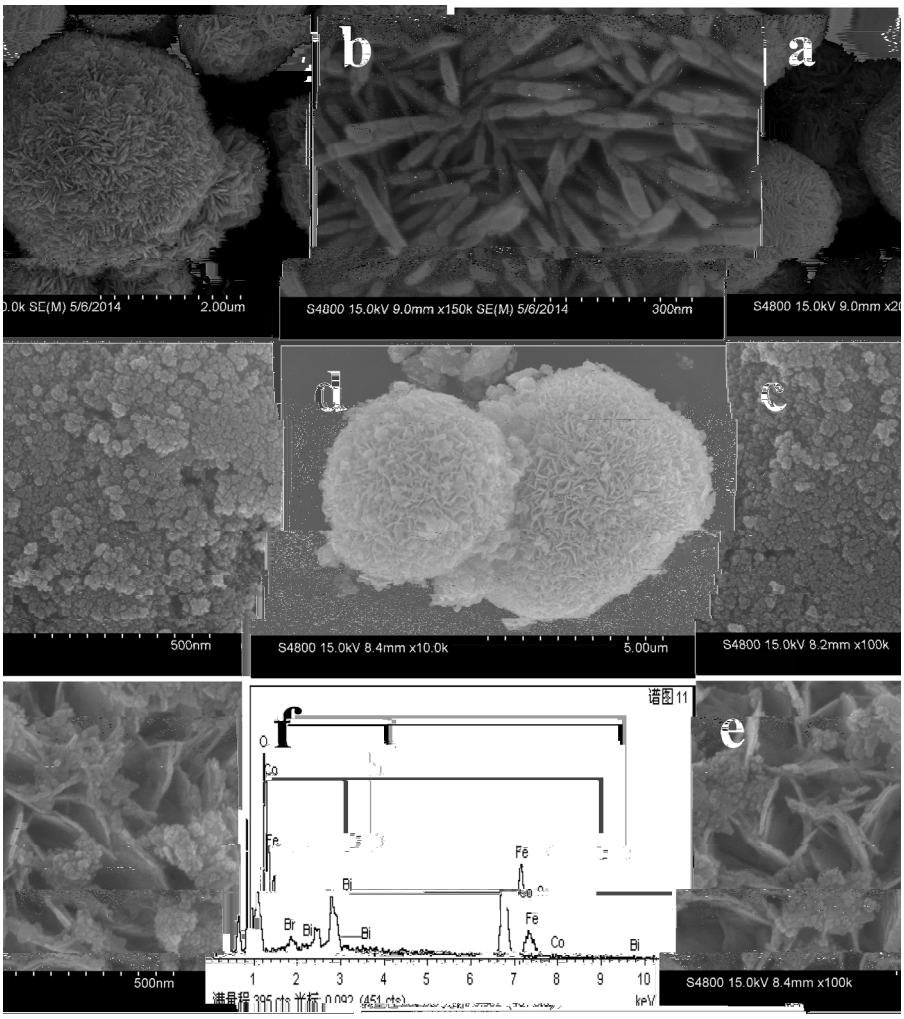

Fig. 4. SEM images of the pure BiOBr (a and b), the pure $CoFe_2O_4$ (c), the hierarchical heterostructured BiOBr/$CoFe_2O_4$ microspheres (d and e) and the EDS of BiOBr/$CoFe_2O_4$ microspheres.

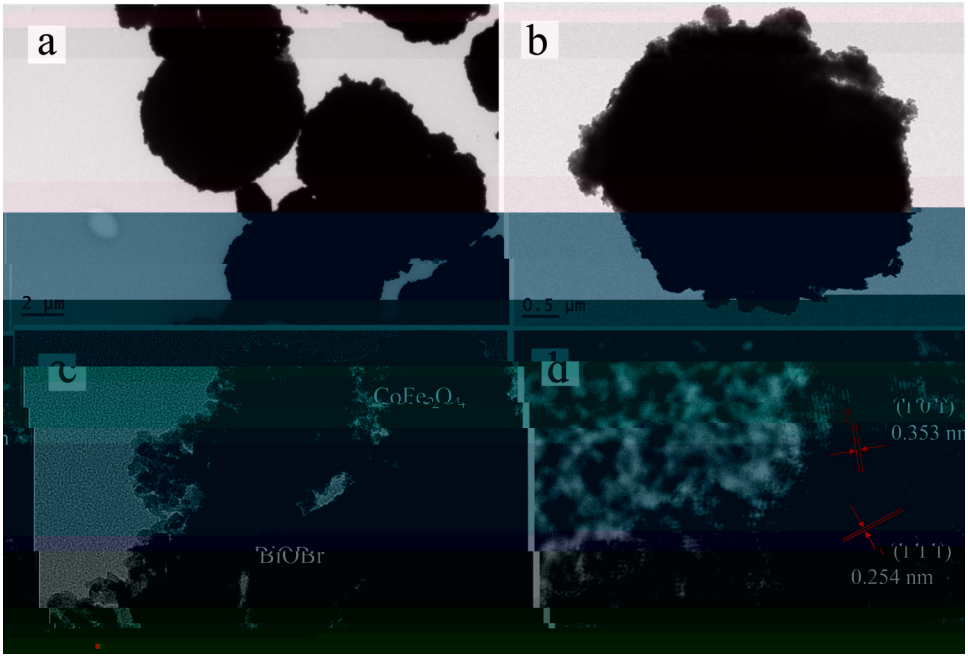

Fig. 5. TEM images of BiOBr/$CoFe_2O_4$ microspheres.

waxberry-like BiOBr microspheres were stuck with some tiny nanoparticles, indicating that $CoFe_2O_4$ nanoparticles have been interspersed on BiOBr microsphere. The existence of $CoFe_2O_4$ nanoparticles could facilitate the separation of the photoinduced electron–hole pairs effectively [34] and convenient recovery from treated solution [30,39]. Those rough surfaces of the BiOBr/$CoFe_2O_4$ microsphere enlarge their surface areas and provide more sizes for adsorption of pollutant

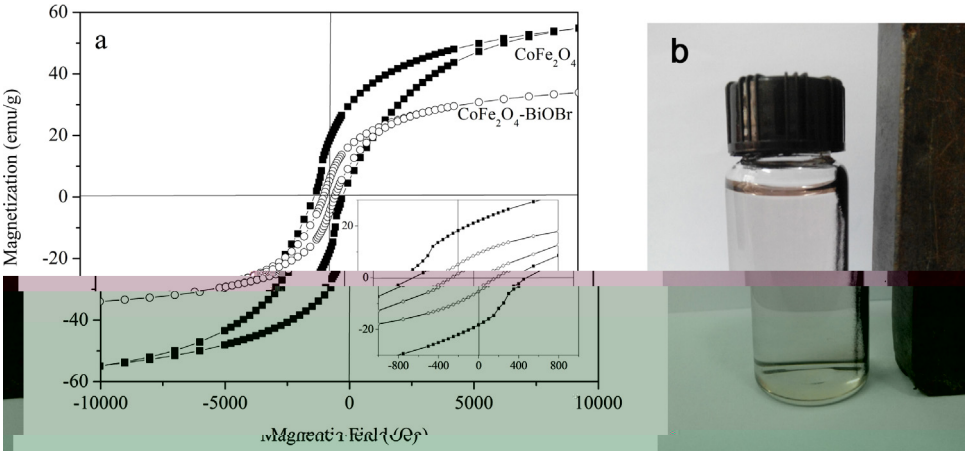

Fig. 7. (a) Magnetization curves of $CoFe_2O_4$, the $BiOBr/CoFe_2O_4$ microspheres measured at room temperature (the inset is the corresponding magnetization of the low field (−2000 to 2000 Oe)) and (b) the separation of $BiOBr/CoFe_2O_4$ microspheres by a magnet.

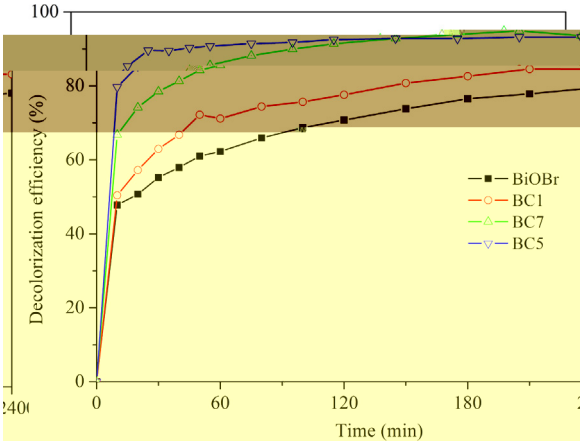

Fig. 8. Comparison of photocatalytic activities of BiOBr, and $BiOBr/CoFe_2O_4$ microspheres on the decolorization of CR solution under simulated solar light irradiation.

as high as that of the pure BiOBr ($0.0650\ min^{-1}$), which results from superior adsorption and transfer performance to organic contaminants in aqueous systems [31]. Considering high efficiency, low price and expectant magnetic performance, $BiOBr/CoFe_2O_4$ weight ratio is controlled in 5:5 for the subsequent photocatalysis decolorization of CR dye by $BiOBr/CoFe_2O_4$ microspheres.

3.3. Effect of initial CR concentration and photocatalyst dosage

It is important to study the dependence of photocatalytic decolorization efficiency on initial pollutant concentration and photocatalyst dosage from an application standpoint of view [56]. Different amounts of $BiOBr/CoFe_2O_4$ microspheres ranging from $0.33\ g\ L^{-1}$ to $1.67\ g\ L^{-1}$ for $15\ mg\ L^{-1}$ CR solutions were employed in this study and the corresponding result is shown in Fig. 9a. An obvious increase of decolorization efficiency of CR solution is observed with the increase of photocatalyst amount from $0.33\ g\ L^{-1}$ to $1.0\ g\ L^{-1}$. However, further increase of catalyst amount over $1.0\ g\ L^{-1}$ causes fewer enhancements on decolorization efficiency of CR by $BiOBr/CoFe_2O_4$ microspheres. The reaction rate constants were calculated from the linear fits of each logarithmic plot of decolorization efficiency as a function of irradiation time. As photocatalyst dosage increased from $0.33\ g\ L^{-1}$ to $1.0\ g\ L^{-1}$ the decolorization kinetic rate constant increased obviously, and reached $0.0135\ min^{-1}$ when photocatalyst dosage was $1.0\ g\ L^{-1}$. The increase of photocatalyst dosage increased the number of

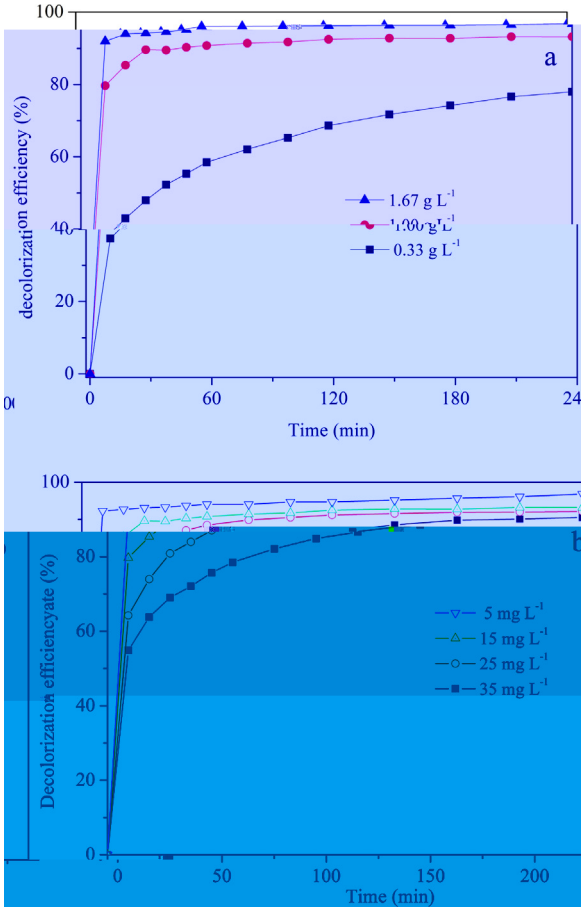

Fig. 9. Effects of catalyst dosage (a) and initial concentration (b) on decolorization efficiency of CR solution under simulated solar light irradiation.

active sites, consequently both absorbed dye molecules and photons increased [3]. However, at higher photocatalyst dosage beyond $1.0\ g\ L^{-1}$, the rate constant increase is not obvious due to the hindrance and blocking of simulated solar light penetration caused by the excessive amount of photocatalyst. From the viewpoint of practical application, the optimum dosage of $BiOBr/CoFe_2O_4$ microspheres ($1.0\ g\ L^{-1}$) for a given concentration of $15\ mg\ L^{-1}$ of CR solution is moderate. Effects of the initial CR concentration on the decolorization efficiency by the $BiOBr/CoFe_2O_4$

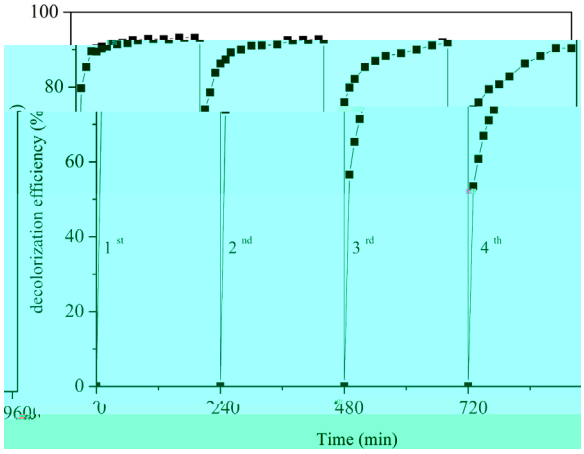

Fig. 10. Cycling runs in the photocatalytic degradation of CR in the presence of $BiOBr/CoFe_2O_4$ microspheres under simulated solar light irradiation.

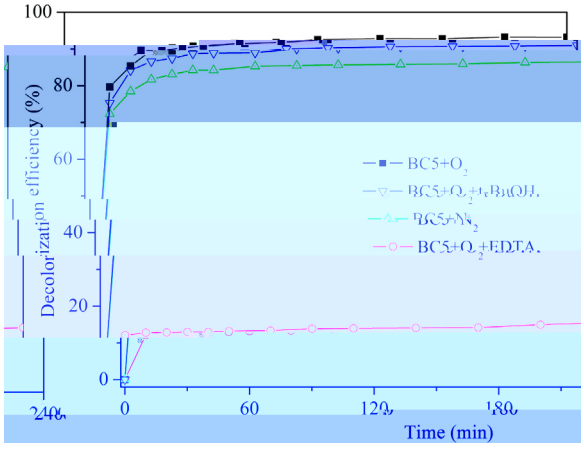

Fig. 11. Photocatalytic decolorization of CR over the $BiOBr/CoFe_2O_4$ microspheres in the present of different scavengers under simulated light irradiation.

microspheres were investigated. Fig. 9b shows the effect of initial CR concentration on photocatalytic decolorization in the presence of 1.0 g L^{-1} $BiOBr/CoFe_2O_4$ microspheres at natural pH. With the increase of initial dye concentration, the decolorization efficiency decreased. The possible explanation is that as the initial concentration of CR increases, the path length of the photons entering the solution decreases. At lower concentration the reversal effect occurred, thereby increasing the number of photon absorbed by $BiOBr/CoFe_2O_4$ microspheres.

3.4. Photocatalytic stability of the photocatalysts

In consideration of practical applications, the photocatalyst should be chemically and optically stable after several repeated trials [57]. The circulating runs in the photocatalytic degradation of CR in the presence of $BiOBr/CoFe_2O_4$ microspheres under simulated solar light were taken to evaluate the stability. Fig. 10 showed the results of CR degradations for four runs. $BiOBr/CoFe_2O_4$ microspheres exhibit remarkable photostability as the CR decolorization efficiency are 93.20%, 92.73%, 91.92%, and 90.36% in the first, second, third, and forth run, respectively. The decrease in the activity of the photocatalyst is only 2.84% after four runs; hence, $BiOBr/CoFe_2O_4$ microspheres can be recycled and reused, which means the photocatalytic decolorization process can be operated in a relatively low cost.

3.5. Role of active species and photocatalytic mechanism

The active species such as trapped holes (h^+), superoxide radical ($O_2^{\bullet-}$) and hydroxyl radical ($^\bullet$OH) are always considered to be the main reasons for the photodegradation of organic pollutant [4,13,58]. For detecting the main active species during photocatalytic reaction, hydroxyl radical ($^\bullet$OH), hole (h^+), and $O_2^{\bullet-}$ were investigated by adding t-BuOH (a quencher of radical scavenger), EDTA-2Na (holes scavenger) and N_2 ($O_2^{\bullet-}$ scavenger), respectively [27]. As shown in Fig. 11, the decolorization efficiency of CR solution decreases notably with the addition of EDTA-2Na compared with that either in the presence of t-BuOH or no addition, indicating that holes are the main reactive species for the photocatalytic decolorization efficiency of CR solution by $BiOBr/CoFe_2O_4$ microspheres [26]. According to previous literature, the conduction band (CB) and valence band (VB) potentials of BiOBr are 0.27 and 3.19 eV, respectively. Therefore, the BiOBr-based photocatalytic reaction under visible light irradiation occurs through the direct oxidation of photogenerated hole with the substrates since it is insufficient for the photogenerated valence band hole of BiOBr to oxidize water to $^\bullet$OH

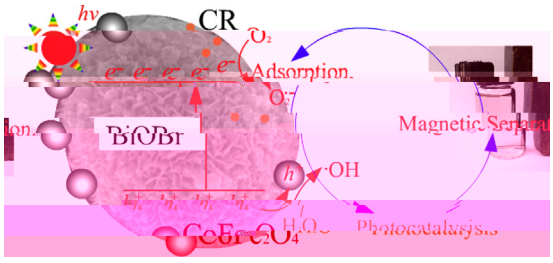

Fig. 12. Schematic diagram of dye decolorization by $BiOBr/CoFe_2O_4$ microspheres under simulated solar light irradiation.

[59]. To test the role of the dissolved oxygen in the degradation process, enough nitrogen (N_2) was bubbled into the suspension to ensure that the reaction system was operated under anoxic conditions. In the presence of N_2, photocatalytic decolorization of CR solution was inhibited compared with that in the presence of O_2 under the same conditions. The result indicated that $O_2^{\bullet-}$ radicals play a role in the photocatalytic decolorization of CR solution by $BiOBr/CoFe_2O_4$ microspheres since $O_2^{\bullet-}$ radicals can be formatted via direct reduction of dissolved oxygen [27]. In a word, the h^+ radicals and $O_2^{\bullet-}$ radicals are considered the two main active species that drive the photodegradation of organic pollutant by $BiOBr/CoFe_2O_4$ microspheres under simulated solar light irradiation.

Based on the above discussion, the possible mechanism of decolorization of CR solution by $BiOBr/CoFe_2O_4$ microspheres has been established and discussed. As shown in Fig. 12, CR molecules were firstly adsorbed fast by $BiOBr/CoFe_2O_4$ microspheres (Eq. (2)) [14,39,60], which led to occur a dye-sensitized reaction of semiconductor [61]. At the same time, the dye-sensitized BiOBr semiconductors in $BiOBr/CoFe_2O_4$ microspheres were excited by simulated solar light irradiation, which induced the generation of electron–hole (e^-/h^+) pairs (Eq. (3)) [11]. The presence of $CoFe_2O_4$ of $BiOBr/CoFe_2O_4$ microspheres led to a more efficient charge separation from BiOBr semiconductor since the introduction of $CoFe_2O_4$ can enhance the photoluminescent intensity of metal oxides (Eq. (4)) [62,63]. Following, the migrated e^- reacted with the oxygen molecule (O_2) that dissolved in aqueous solution to generate $O_2^{\bullet-}$ (Eq. (5)) [64]. The part h^+ radicals reacted with H_2O molecules in solution to generate reactive hydroxyl ($^\bullet$OH) and H^+ ions (Eq. (6)) [12]. Then the photoinduced holes (h^+) directly oxidized the CR dye pollutants to generate the activated CR^+, which then reacted with generated $O_2^{\bullet-}$ radicals or $^\bullet$OH radicals to generate H_2O, CO_2 and other small ultimate byproducts (Eqs. (8) and (9)).

Generally speaking, Eqs. (2), (3), (7) and (8) are the main reaction since the h^+ and $O_2^{\bullet-}$ radicals are the two main active species according to the radical trapping experiments. After magnetic separation, BiOBr/$CoFe_2O_4$ microspheres can be reused to treat other

tCatal tBTj/F21Tf.000200-.0002252.838694.29369Tm0g()Tj/F11Tf6.3761006.3761129404252694.2932Tm0g502.675rg(t165Tj/F21Tf.00

[36] F. Sadri, A. Ramazani, A. Massoudi, M. Khoobi, V. Azizkhani, R. Tarasi, L. Dolatyari, B.K. Min, Magnetic $CoFe_2O_4$ nanoparticles as an efficient catalyst for the oxidation of alcohols to carbonyl compounds in the presence of oxone as an oxidant, Bull. Korean Chem. Soc. 35 (2014) 2029–2032.
[37] Q. Song, Z.J. Zhang, Shape control and associated magnetic properties of spinel cobalt ferrite nanocrystals, J. Am. Chem. Soc. 126 (2004) 6164–6168.
[38] R.S. Yadav, J. Havlica, J. Masilko, L. Kalina, M. Hajdúchová, V. Enev, J. Wasserbauer, I. Kuritka, Z. Kozakova, Structural, cation distribution, and magnetic properties of $CoFe_2O_4$ spinel ferrite nanoparticles synthesized using a starch-assisted sol–gel auto-combustion method, J. Supercond. Nov. Magn. 28 (2015) 1851–1861.
[39] M.A. Khan, M.M. Alam, M. Naushad, Z.A. Alothman, M. Kumar, T. Ahamad, Sol-gel assisted synthesis of porous nano-crystalline $CoFe_2O_4$ composite and its application in the removal of brilliant blue-R from aqueous phase: an eco-friendly and economical approach, Chem. Eng. J. 279 (2015) 416–424.
[40] Y. Ren, L. Lin, J. Ma, J. Yang, J. Feng, Z. Fan, Sulfate radicals indTm/F2-.0002158.0101714.0284Tm0ga31658.2372Tm0g()Tj/F11Tf6.3761006.37612189.9888658.2372Tm0.502.675rg(ir
bu

《SCI-Expanded》收录及《JCR》期刊影响因子证明

经检索《Web of Science》和《Journal Citation Reports（JCR）》数据库，《Science Citation Index Expanded (SCI-EXPANDED)》收录论文及其期刊影响因子如下：（检索